Cooling of a Hot Stretching Surface in the Presence of Across Mass Transfer Phenomenon in a Channel Flow

Ahmer Mehmood[a], Sufian Munawar[b,c], and Asif Ali[c]

[a] Department of Mathematics (FBAS), International Islamic University Islamabad, Pakistan
[b] Department of Mathematics (SST), University of Management and Technology Lahore, Pakistan
[c] Department of Mathematics Quaid-i-Azam University Islamabad, Pakistan

Reprint requests to S. M.; E-mail: sufian.munawar@hotmail.com

Z. Naturforsch. **69a,** 34 – 42 (2014) / DOI: 10.5560/ZNA.2013-0070
Received May 28, 2013 / revised September 13, 2013 / published online December 4, 2013

This is an attempt to investigate the best possible flow situation in order to optimize the rate of heat exchange between the stretching plate and the ambient fluid. The generalized three-dimensional channel flow of an incompressible viscous fluid has been considered where both the walls of the channel are assumed to be porous and the lower wall stretching in two lateral directions at different rates. The effect of simultaneous suction and injection at the lower and upper walls, respectively (and vice versa), have been studied in detail. It is named as across mass transfer phenomenon (AMT). It is observed that even in the presence of viscous dissipation the across mass transfer increases the rate of heat exchange from plate to fluid. A purely analytic solution has been obtained by homotopy analysis method and results are also compared with a numerical technique. Results are discussed through graphs.

Key words: Three-Dimensional Channel Flow; Across Mass Transfer; Heat Transfer.

1. Introduction

Due to its important applications in polymer industry, the study of heat transfer phenomenon from a stretching sheet to the ambient fluid has grown considerably. A lot of literature has been devoted to the investigation of best suited flow assumptions which can yield a maximum rate of heat exchange from the hot surface to the surrounding fluid. In these studies, the researchers had been trying their luck by considering different flow geometries or by introducing some other physical features such as suction/injection, magnetohydrodynamics (MHD), introduction of a porous medium etc. In all such practices, people have been successfully attempted to avoid the delay in heat transfer but still there is a room for better proposals.

Heat transfer analysis of a viscous flow over a stretching sheet was first studied by Crane [1] who considered a two-dimensional boundary-layer flow of a viscous fluid over a stretching sheet and presented a closed form solution. Afterwards, Gupta and Gupta [2] studied the effects of wall suction/injection on the heat transfer phenomenon as studied by Crane. In 1982, Carragher and Crane [3] investigated the heat transfer analysis in a viscous fluid by taking the temperature difference between the hot wall and the ambient fluid proportional to the distance from a fixed point. Banks and Zaturska [4] obtained eigen solutions to the boundary-layer flow over a stretching sheet. Further contribution on the heat transfer analysis can be found in Chen and Char [5], Dandapat and Gupta [6], Dutta et al. [7], Mehmood et al. [8], Elbashbeshy [9], Grubka and Bobba [10], Mehmood and Ali [11], and Liao and Campo [12]. In all the above mentioned studies, the authors considered a two-dimensional flow. However, the literature lacks in providing a sufficient material on three-dimensional flows with heat transfer phenomenon but still there are some significant contributions present in literature such as; Lakshmisha et al. [13], Aboeldahab and Azzam [14], Mehmood and Ali [15], Takhar et al. [16] etc. The authors considered unbounded domains in these studies. However, there are studies in which authors have tried the channel flow in order to improve the heat transfer phenomenon. In 1983, Borkakoti and Bharali [17] investigated the hydromagnetic flow with heat transfer

analysis in a channel with lower wall as a stretching sheet. Mehmood and Ali [18] investigated the three-dimensional flow with heat transfer in a channel of lower stretching wall in a rotating frame of reference. Munawar et al. [19] investigated the effect of squeezing on the hydromagnetic flow in a rotating channel of lower stretching wall. Recently, Mehmood and Ali [20] discussed the three-dimensional flow in a porous channel of lower stretching wall. The authors introduced the phenomenon of *across mass transfer* (AMT) by taking injection at upper plate and suction at the lower one. In [20], authors showed that viscous drag on the lower stretching sheet can be reduced by introducing AMT phenomenon. Moreover, Mehmood and Ali [21] investigated the heat transfer analysis in a generalized three-dimensional flow of a viscous fluid in a channel of lower stretching wall assuming the upper wall of the channel as a porous sheet subjected to uniform injection. Further in [21], the authors have also investigated the effect of viscous dissipation on the process of cooling of the sheet, and it was observed that cooling of the sheet is possible only if the viscous dissipation is very small. Therefore, it is required to device some suitable flow assumptions under which the effect of viscous dissipation can be reduced so that the stretching sheet can be cooled efficiently in the presence of viscous dissipation. In order to expedite the cooling process of the sheet, we have replaced the lower non-porous stretching wall of the channel by a porous one. In this way, the mass can be transferred to and from the channel through both the plates and especially the AMT can take place in this situation. In our study, we classify the phenomenon of mass transfer into two classes, namely, when both the plates are subjected to the same phenomenon (viz. suction or injection) or when both the walls are subjected to the opposite phenomenon (viz. suction and injection simultaneously). In the former case, the fluid is either injected to or sucked from the channel but in later case, the mass is injected from one plate and is sucked from the other, that means, the mass is actually transferred across the channel. Useful contribution of the AMT phenomenon on the heat transfer rate has been observed in this study.

We present a purely analytic and highly accurate solution to the governing nonlinear equations of the considered problem. The accuracy of present results has been shown by calculating the residual errors and comparing the result by a numerical scheme. We have used the homotopy analysis method (HAM) [22] to solve the governing nonlinear system analytically. The homotopy analysis method has a great potential of dealing with highly nonlinear problems with great comfort, and there are a number of problems in literature in which the authors have used HAM as their solution technique. Some significant contributions can be found in Liao [23, 24], Liao and Cheung [25], Wang et al. [26], Tan and Abbasbandy [27], Bararnia et al. [28], Moghaddam et al. [29], Abbas and Hayat [30], Mehmood et al. [31], and Munawar et al. [32].

2. Mathematical Description

We consider an incompressible viscous fluid bounded by two infinite parallel flat plates situated at $z=0$ and $z=h$ as considered in [20]. It is assumed that the lower plate is heated at a constant temperature θ_0, and the upper plate is fixed at temperature θ_h such that $\theta_0 > \theta_h$. In this case, the governing system comprises of the continuity equation, the Navier–Stokes equations as given in [20], and the energy equation given by

$$\begin{aligned} u\frac{\partial\theta}{\partial x}+v\frac{\partial\theta}{\partial y}+w\frac{\partial\theta}{\partial z} &= k\left(\frac{\partial^2\theta}{\partial x^2}+\frac{\partial^2\theta}{\partial y^2}+\frac{\partial^2\theta}{\partial z^2}\right) \\ &+\frac{\nu}{C_p}\left[\left(\frac{\partial u}{\partial y}+\frac{\partial v}{\partial x}\right)^2+\left(\frac{\partial u}{\partial z}+\frac{\partial w}{\partial x}\right)^2\right. \\ &+\left(\frac{\partial v}{\partial z}+\frac{\partial w}{\partial y}\right)^2+2\left(\left(\frac{\partial u}{\partial x}\right)^2+\left(\frac{\partial v}{\partial y}\right)^2\right. \\ &\left.\left.+\left(\frac{\partial w}{\partial z}\right)^2\right)\right], \end{aligned} \tag{1}$$

with the suitable boundary conditions

$$\theta=\theta_0 \text{ at } z=0 \text{ and } \theta=\theta_h \text{ at } z=h, \tag{2}$$

where u, v, and w are the velocity components, x, y, and z are the space variables. Further are ν the viscosity and k the thermal diffusivity of the fluid; C_p is the specific heat, h the width of the channel, θ_0 the temperature at the lower wall, and θ_h the temperature at the upper wall. We introduce the similarity transformations

$$\begin{aligned} &\eta=\frac{1}{h}z,\ u=axf'(\eta),\ v=ayg'(\eta), \\ &w=-ah(f+g),\ T(\eta)=\frac{\theta-\theta_h}{\theta_0-\theta_h}, \end{aligned} \tag{3}$$

due to which (1) after some mathematical simplifications transforms to

$$T'' = \Pr\Big[\mathrm{Re}(f+g)T' + 4\mathrm{Ec}\,\mathrm{Re}\left(f'^2+g'^2+f'g'\right)+\mathrm{Ec}_x f''^2+\mathrm{Ec}_y g''^2\Big] \tag{4}$$

with the transformed boundary conditions

$$T(0)=1\,,\;\; T(1)=0\,, \tag{5}$$

where $'$ denotes the differentiation with respect to η, $\mathrm{Re}=ah^2/\nu$ is the Reynolds number, $\Pr=\mu C_p/k$, is the Prandtl number, $\mathrm{Ec}=\nu a/C_p(\theta_w-\theta_0)$ is the Eckert number, $\mathrm{Ec}_x=a^2x^2/C_p(\theta_w-\theta_0)$ and $\mathrm{Ec}_y=a^2y^2/C_p(\theta_w-\theta_0)$ are the local Eckert numbers based on the lateral and the vertical axes, respectively. At this stage it is useful to remind that the flow analysis for the present problem has already been discussed in detail in [20]. In this study, we shall focus on the heat transfer phenomenon. Therefore the equations and boundary conditions for the involved velocity components have not been given here in order to make the manuscript compact. However, we shall also be solving those equations while solving (4) and (5) in the present case.

3. Solution of the Problem

3.1. Analytic HAM Solution

Before starting the solution process, it is important to mention that our governing system consists of (7)–(9) of [20] and (4) and (5) of the present study. In order to get the temperature profile, we shall have to solve the full governing system. However, in the solution procedure we shall only be talking about (4) and (5) as the solution procedure for the system (7)–(9) of [20] has already been given in [20]. The reader is referred to this reference for solution details of the system (7)–(9) in [20].

We use HAM to solve the governing system and choose the initial guess approximations satisfying the boundary conditions (5) as follows:

$$T_0(\eta)=1-\eta\,. \tag{6}$$

In view of the boundary conditions (5), we choose the linear operator as

$$\mathcal{L}_T \equiv \frac{\mathrm{d}^2}{\mathrm{d}\eta^2}\,. \tag{7}$$

Since the homotopy analysis method is well known and is widely used by the community of fluid dynamics and heat and mass transfer, it seems appropriate to not repeat all the procedural details of the method here again. However, the reader can consult references [20] and [23–32] for details of the HAM solution procedure. We therefore directly write the mth-order deformation equation ($m\geq 1$) given by

$$\mathcal{L}_T\left[T_m(\eta)-\chi_m T_{m-1}(\eta)\right]=\hbar H_m(\eta)\,, \tag{8}$$

subject to the boundary conditions

$$T_m(0)=1\,,\;\; T_m(1)=0\,, \tag{9}$$

where

$$\begin{aligned} H_m(\eta) &= T''_{m-1}(\eta) \\ &+\Pr\mathrm{Re}\sum_{k=0}^{m-1}\left(f_{m-1-k}(\eta)+g_{m-1-k}(\eta)\right)T'_k \\ &+4\mathrm{Ec}\,\Pr\mathrm{Re}\sum_{k=0}^{m-1}\left(f'_{m-1-k}f'_k+g'_{m-1-k}g'_k+f'_{m-1-k}g'_k\right) \\ &+\Pr\mathrm{Ec}_x\sum_{k=0}^{m-1}f''_{m-1-k}(\eta)\,f''_k(\eta) \\ &+\Pr\mathrm{Ec}_y\sum_{k=0}^{m-1}g''_{m-1-k}(\eta)\,g''_k(\eta)\,, \end{aligned} \tag{10}$$

and

$$\chi_k=\begin{cases}0 & \text{for } k\leq 1,\\ 1 & \text{for } k>1.\end{cases}$$

Clearly, for a particular value of 'm', (8) is an ordinary differential equation which could easily be solved by a standard method. In this way, the final solution can be written in the form of an infinite series of functions:

$$T(\eta)=T_0(\eta)+\sum_{m=1}^{\infty}T_m(\eta)\,, \tag{11}$$

where $T_m(\eta)$ is the solution of the mth-order ($m\geq 1$) deformation equation.

3.2. Convergence of HAM Solution

As mentioned by Liao [22], the convergence of the HAM solution series strongly depends upon the value of the convergence controlling parameter, namely, $\hbar$. The suitable value of this parameter has been found by plotting the squared residual error for (4) against the convergence controlling parameter. The value cor-

Order	$-f''(0)$	$\Delta f_i''(0)$	$-g''(0)$	$\Delta g_i''(0)$	$-T'(0)$	$\Delta T_i'(0)$
5^{th}	4.76572	$6.41208\cdot10^{-6}$	2.35574	$3.17298\cdot10^{-6}$	0.720517	$8.20285\cdot10^{-5}$
10^{th}	4.76606	$1.45755\cdot10^{-9}$	2.35591	$6.91880\cdot10^{-10}$	0.720055	$2.96560\cdot10^{-8}$
15^{th}	4.76606	$3.06068\cdot10^{-13}$	2.35591	$1.03716\cdot10^{-13}$	0.720055	$4.46887\cdot10^{-12}$
20^{th}	4.76606	$2.08522\cdot10^{-16}$	2.35591	$8.82251\cdot10^{-17}$	0.720055	$4.99412\cdot10^{-15}$

Table 1. HAM solution and squared residual error at different orders of approximation when $\hbar = -0.8$, $\mathrm{Re} = 2$, $\beta = w_0 = w_1 = 0.5$, $\mathrm{Ec} = \mathrm{Ec}_x = \mathrm{Ec}_y = 0.2$ are kept fixed.

Re	β	$w_0 = w_1$	$-f''(0)$ HAM	$-f''(0)$ Numerical	$-g''(0)$ HAM	$-g''(0)$ Numerical	$T'(0)$ HAM	$T'(0)$ Numerical
1	0.5	0.5	4.368753	4.368753	2.169674	2.169674	−0.576330	−0.576330
2			4.766056	4.766056	2.355906	2.355906	−0.720055	−0.720055
3			5.182701	5.182701	2.556487	2.556487	−0.895818	−0.895818
2	0.5		4.766056	4.766056	2.355906	2.355906	−0.720055	−0.720055
	1		4.768951	4.768951	2.355900	2.355900	−0.719978	−0.719978
	2		4.823284	4.823284	4.801888	4.801888	−0.256281	−0.256281
2	0.5	−0.5	3.872515	3.872515	7.820793	7.820793	1.924566	1.924566
		0.0	4.108416	4.108416	2.072480	2.072480	−0.365235	−0.365235
		0.5	4.766056	4.766056	2.355906	2.355906	−0.720055	−0.720055

Table 2. Comparison of HAM solution with numerical shooting method when $\hbar = -0.8$, $\mathrm{Pr} = 0.71$, $\mathrm{Ec} = \mathrm{Ec}_x = \mathrm{Ec}_y = 0.2$ are kept fixed.

responding to the minimum residual error is regarded as the optimal value of $\hbar$. To choose this optimal value, we minimize the squared residual error using the first derivative law of Calculus and plotted the error against $\hbar$ in Figure 1. Clearly, at $\hbar = -0.8$ (roughly) the squared residual error graph touches the zero (see Fig. 1). From here we can choose an appropriate guess for the convergence controlling parameter. We have shown the convergence of our solution by calculating the solutions at different orders of approximation in Table 1. In HAM solution series (11), the higher orders of approximation are the corrections to the solution, and for a convergent series the corrections must die out on increasing the order of approximations. We have also calculated such kind of corrections (see Table 1) for the present problem at different orders of approximation by calculating the differences $\Delta f_i''(0) = |f_i''(0) - f_{i-1}''(0)|$, $\Delta g_i''(0) = |g_i''(0) - g_{i-1}''(0)|$ and $\Delta T_i'(0) = |T_i'(0) - T_{i-1}'(0)|$. From Table 1 it is also clear that the corrections to the HAM solution become negligible at higher orders of approximations. This proves the convergence of our HAM solution.

4. Numerical Solution

In order to validate our analytic solution, we again solve the boundary value problem (4) and (5) numerically with the help of the shooting method using the integrated commands of computational software *Mathematica*. To preserve the best precision of numerical algorithm, we adjust the working precision to 120 decimal places for the entire algorithm. Setting accuracy-

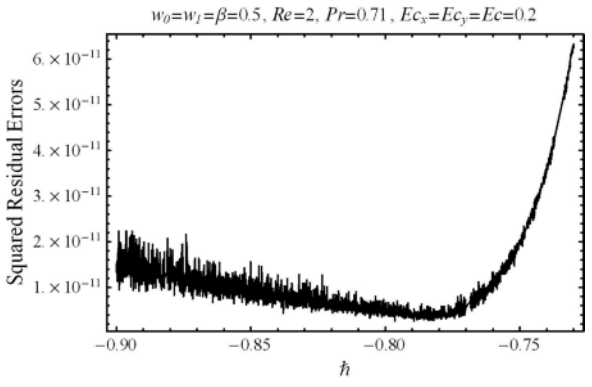

Fig. 1. Residual error against $\hbar$ at 20^{th}-order of approximation.

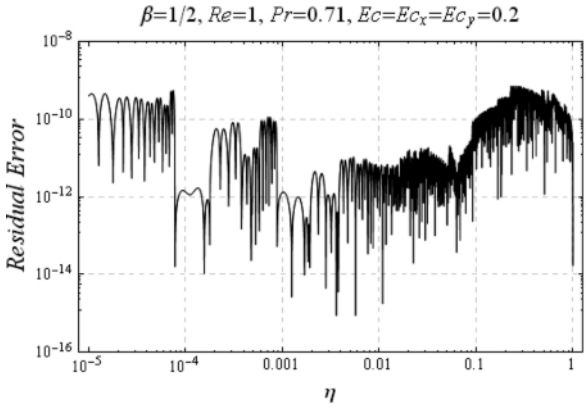

Fig. 2. Residual error in the numerical solution by shooting method.

goal equals to 20 decimal places and precision-goal equals to 40 decimal places, we get the numerical solution of the desired accuracy. This means that the software attempts to make the numerical error in a result of size k be less than $10^{-20}+|k|10^{-40}$. Figure 2 shows the residual error graphs for (4) by fixing the other parameters. The figure illustrates that the error is in admissible range which shows that our numerical scheme offers a highly accurate solution. A comparison has been made in Table 2 for both solution methodologies to validate our present solutions. The table depicts the values of $f''(0)$, $g''(0)$, and $T'(0)$ for various values of the parameters Re, β, w_0, and w_1. From the table it is clear that both the solutions are in good agreement up to six decimal places which proves the accuracy/exactness of our solution.

5. Results and Discussion

In order to investigate the effect of across mass transfer (AMT) on temperature distribution in the channel and on the rate of heat exchange, graphs are plotted in Figures 5 – 14. Notice that in Figures 5 – 14, we have fixed $\beta = 0.5$ and Re $= 2$. In Figures 5 – 10, we have plotted the temperature profiles for the case when the viscous dissipation is assumed to be zero. In Figures 11 – 14 the same graphs have been plotted for the case when viscous dissipation has been taken into account. This in fact helps us to see the effect of AMT phenomenon (in both the cases with and without viscous dissipation) in the process of cooling of the sheet. In Figure 3, we have plotted temperature profile against η at fixed w_1 $(=0)$ for different values of the suction

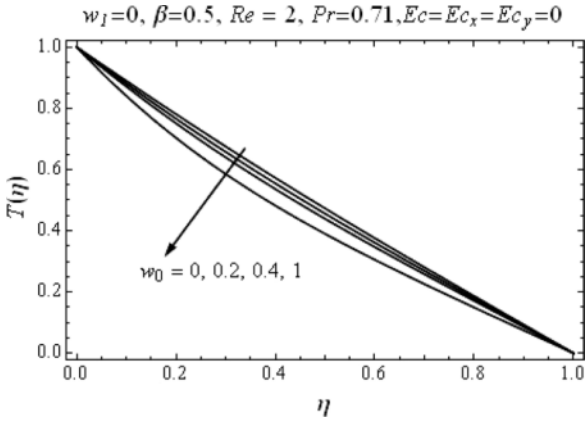

Fig. 3. Temperature $T(\eta)$ at different w_0 when $w_1 = 0$ in the absence of viscous dissipation.

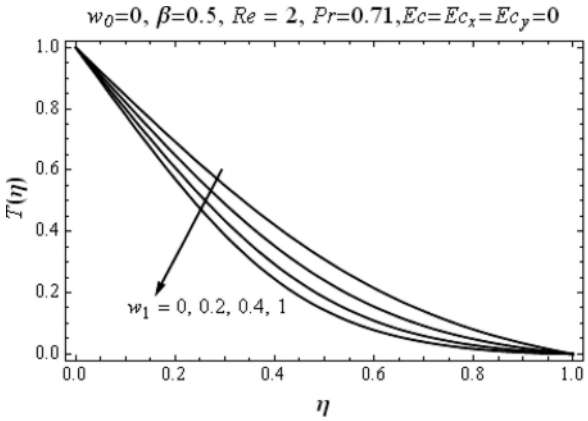

Fig. 4. Temperature $T(\eta)$ at different w_1 when $w_0 = 0$ in the absence of viscous dissipation.

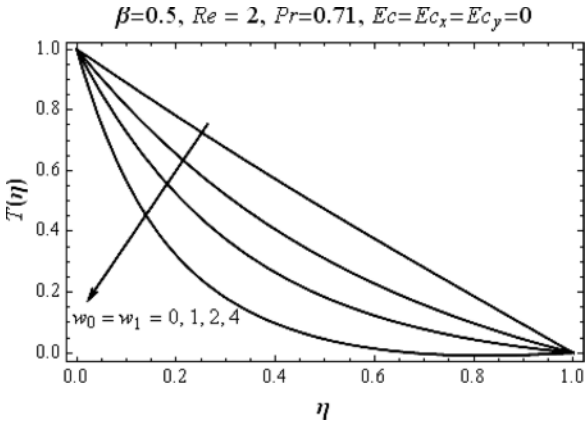

Fig. 5. Temperature $T(\eta)$ in the presence of AMT applied downwards in the absence of viscous dissipation.

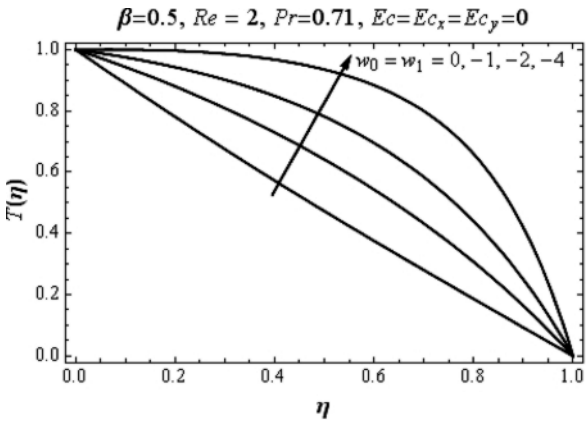

Fig. 6. Temperature $T(\eta)$ in the presence of AMT applied upwards in the absence of viscous dissipation.

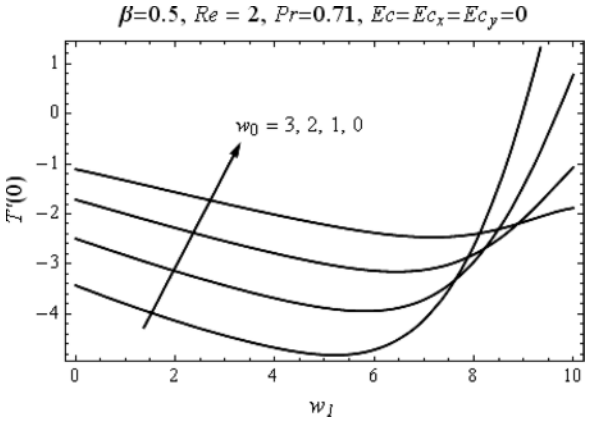

Fig. 7. $T'(0)$ plotted against w_1 in the absence of viscous dissipation.

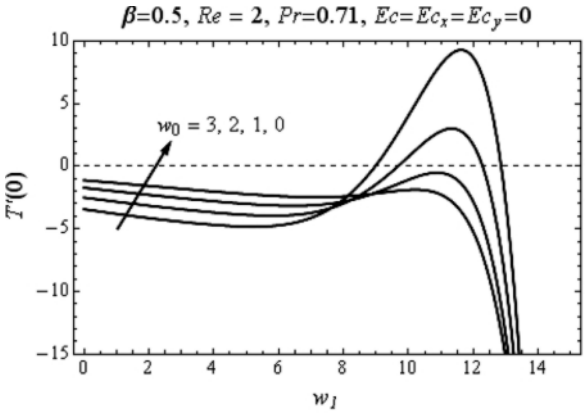

Fig. 8. $T'(0)$ plotted against w_1 in the absence of viscous dissipation.

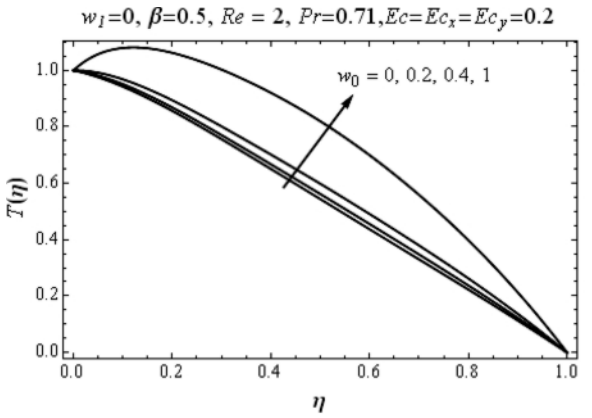

Fig. 9. Temperature $T(\eta)$ at different w_0 when $w_1 = 0$ in the presence of viscous dissipation.

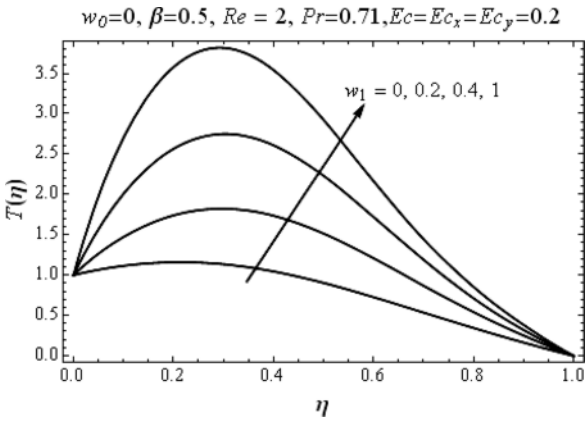

Fig. 10. Temperature $T(\eta)$ at different w_1 when $w_0 = 0$ in the presence of viscous dissipation.

parameter w_0. Clearly, in the absence of mass transfer at the upper wall, the suction at the lower plate causes to enhance the cooling process but this effect is very little. In contrast, we have plotted the temperature profile at fixed w_0 $(= 0)$ for different values of the upper wall injection parameter w_1 in Figure 4. Here the upper wall injection increases the rate of heat transfer by reducing the temperature of the fluid bounded between the two plates. This is because due to the upper wall injection the fresh fluid enters in the channel and causes a temperature reduction. A comparison of Figures 3 and 4 reveals that the effect of the upper wall injection is stronger than that of the lower wall suction, but it must be noted that both the phenomenon contribute to enhance the cooling process. In this way it is natural to try both the situations (of Figs. 3 and 4) simultaneously because it is straightforward to expect a rapid rate of heat exchange as a consequence of the joint effect of w_0 and w_1. To see this effect, we have plotted (in Figs. 7 and 8) the temperature profile in the presence of mass transfer at both the plates (called AMT). Clearly, in the presence of AMT (form the upper wall to lower plate) a significant improvement in the rate of heat exchange can be seen in Figure 5. This is because of the suction at lower plate, the hot fluid near the plate leaves the channel and due to the injection at upper wall, the fresh fluid enters the channel and thus the temperature of inner fluid decreases which causes to enhance the rate of heat exchange. However, if the direction of AMT is reversed (from lower to the upper plate) the temperature increases in the channel happening to depreciate the rate of heat exchange between the heated wall and the surrounding fluid (see Fig. 6). The reason is that the injection at the lower wall increases

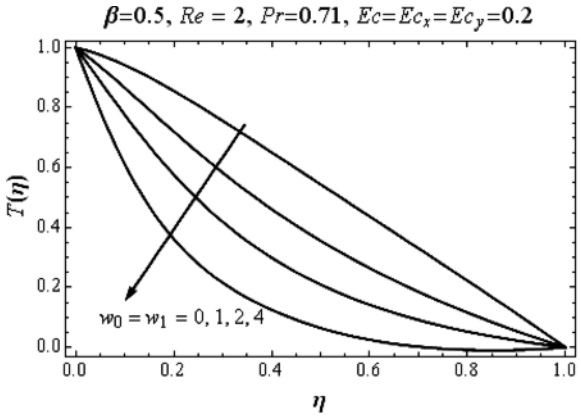

Fig. 11. Temperature $T(\eta)$ in the presence of AMT applied downwards in the presence of viscous dissipation.

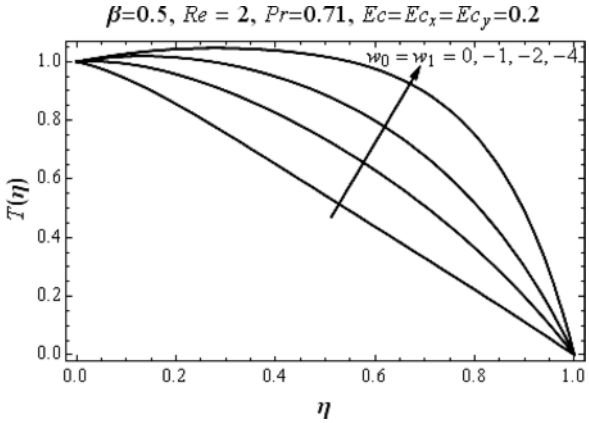

Fig. 12. Temperature $T(\eta)$ in the presence of AMT applied upwards in the presence of viscous dissipation.

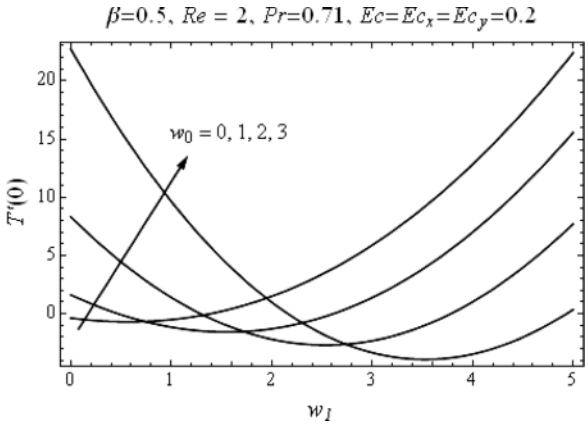

Fig. 13. $T'(0)$ plotted against w_1 in the presence of viscous dissipation.

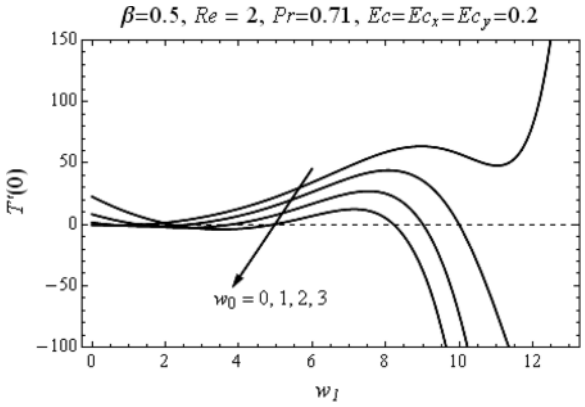

Fig. 14. $T'(0)$ plotted against w_1 in the presence of viscous dissipation.

the thickness of the thermal boundary layers due to which the temperature is encouraged to spread in the channel resulting in a low rate of heat exchange. Thus due to Figures 5 and 6, we conclude that only a suitable direction of AMT can be considered in order to expedite the cooling process. In Figures 7 and 8, we have plotted the rate of heat transfer against w_1 for different values of w_0. From the two Figures (Figs. 9 and 10) it is clear that the rate of heat exchange from plate to fluid is increasing in the increasing direction of w_1 but after some fixed values of w_1 the rate of heat exchange decreases. It is observed that for particular values of w_0 there are intervals of values of w_1 for which the cooling process is too week or impossible but on further increasing the values of w_1 the rate of heat exchange from plate to fluid increases significantly. We discuss the reasons of this fact in the coming paragraph.

In Figures 11 – 14, we have plotted the temperature profile in the presence of viscous dissipation. In Figures 11 and 12, the temperature profile for different values of w_0 and w_1 by keeping $w_1 = 0$ and $w_0 = 0$, respectively, is displayed. In both the graphs it is observed that the mass transfer phenomenon at either plate enhances the temperature near the stretching plate and the effect of w_1 is stronger than that of w_0 (see Figs. 9 and 10). This shoot up in temperature is due to the presence of viscous resistance. In Figure 11, we show the temperature graphs to see the effect of AMT by fixing the same values for the parameters w_0 and w_1 (see Fig. 11). Clearly, even in the presence of viscous dissipation AMT enhances the rate of heat exchange by reducing the temperature of the bounded fluid showing that the introduction of AMT is a useful practice to expedite the cooling process. However,

the effects are totally reversed if the direction of AMT is changed as shown in Figure 12. In Figures 13 and 14, we have plotted the rate of heat transfer at the plate against w_1 for different values of w_0. Figure 13 depicts that for a non-porous wall cooling is possible only for small values of w_1, and for large values of w_1, the cooling of the stretching plate is not possible. However, for porous wall subjected to constant suction it is observed that corresponding to each value of w_0 there are two intervals of values for w_1 in which cooling is possible. For example for $w_0 = 0.4$, the first interval of values of w_1 can be obtained from Figure 13 and the other interval can be observed from Figure 14. Similar to the previous case (without viscous dissipation, see Figs. 7 and 8) again in this case a particular interval of values of w_1 corresponding to particular values of w_0 is present for which the cooling is poor or impossible. Such intervals can be observed in Figure 14. This suggests that in the case of AMT a suitable combination of values of w_0 and w_1 must be introduced (for both kinds of heat transfer, namely, with and without viscous dissipation) in order to get a maximum rate of heat exchange.

6. Concluding Remarks

In this study, we have investigated the effect of across mass transfer phenomenon on the temperature distribution in the channel of lower stretching wall heated at constant temperature and on the heat transfer rate from the hot surface to the surrounding fluid. A purely analytic and highly accurate solution has been obtained for the heat transfer flow. The issue of convergence and accuracy of the HAM solution has been discussed in detail. To prove the accuracy of the HAM solution, a comparison has been made with a numerical scheme. AMT phenomenon is observed to be a useful practice in order to avoid the spreading of the heat across the channel in both the cases viz. in the presence of viscous dissipation and in the absence of viscous dissipation. In the presence of viscous dissipation, it is observed that the temperature overshoot near the solid surface can be controlled with the help of AMT. We have observed that in order to establish AMT, a suitable combination of the suction and injection must be introduced because there exist certain combinations of the values of suction and injection parameters for which the cooling is very poor or impossible in both the cases (with and without viscous dissipation).

Acknowledgement

The first author is thankful to the Alexander von Humboldt Foundation for financial support.

[1] L. Crane, Z. Angew. Math. Phys. **21**, 645 (1970).
[2] P. S. Gupta and A. S. Gupta, Can. J. Chem. Eng. **55**, 744 (1977).
[3] P. Carragher and L. J. Crane, Z. Angew. Math. Mech. **62**, 564 (1982).
[4] W. H. H. Banks and M. B. Zaturska, IMA J. Appl. Math. **36**, 263 (1986).
[5] C. K. Chen and M. I. Char, J. Math. Anal. Appl. **135**, 568 (1988).
[6] B. S. Dandapat and A. S. Gupta, Int. J. Nonlin. Mech. **24**, 215 (1989).
[7] B. K. Dutta, P. Roy, and A. S. Gupta, Int. Commun. Heat Mass **12**, 89 (1985).
[8] A. Mehmood, A. Ali, and T. Shah, Commun. Nonlin. Sci. Numer. Simul. **13**, 902 (2008).
[9] E. M. A. Elbashbeshy, J. Phys. D: Appl. Phys. **31**, 1951 (1998).
[10] L. J. Grubka and K. M. Bobba, J. Heat Trans. T.-ASME **107**, 248 (1985).
[11] A. Mehmood and A. Ali, J. Appl. Mech.-T. ASME **75**, 061003 (2008).
[12] S. J. Liao and A. Campo, J. Fluid Mech. **453**, 411 (2002).
[13] K. N. Lakshmisha, S. Venkateswaran, and G. Nath, J. Heat Trans. T.-ASME **110**, 590 (1988).
[14] E. M. Aboeldahab and G. E. D. A. Azzam, Acta Mech. **184**, 121 (2006).
[15] A. Mehmood and A. Ali, Int. Commun. Heat Mass **33**, 1243 (2006).
[16] H. S. Takhar, A. J. Chamkha, and G. Nath, Acta Mech. **146**, 59 (2001).
[17] A. K. Borkakoti and A. Bharali, Q. Appl. Math. **40**, 461 (1982).
[18] A. Mehmood and A. Ali, J. Heat Trans. T.-ASME **130**, 121701 (2008).
[19] S. Munawar, A. Mehmood, and A. Ali, Comput. Math. Appl. **64**, 1575 (2012).
[20] A. Mehmood and A. Ali, Chem. Eng. Commun. **198**, 678 (2011).
[21] A. Mehmood and A. Ali, J. Taiwan Inst. Chem. E. **41**, 29 (2010).

[22] S. J. Liao, Beyond Perturbation: Introduction to the Homotopy Analysis Method, Chapman and Hall/CRC Press, Boca Raton, Florida 2004.
[23] S. J. Liao, Int. J. Heat Mass Trans. **48**, 2529 (2005).
[24] S. J. Liao, J. Fluid Mech. **488**, (2003).
[25] S. J. Liao and K. F. Cheung, J. Eng. Math. **45**, 105 (2003).
[26] C. Wang, J. M. Zhu, S. J. Liao, and I. Pop, Int. J. Heat Mass Trans. **46**, 1855 (2003).
[27] Y. Tan and S. Abbasbandy, Commun. Nonlin. Sci. Numer. Simul. **13**, 539 (2008).
[28] H. Bararnia, G. Domairry, M. Gorji, and A. Rezania, Numer. Meth. Part. D. E. **26**, 1 (2010).
[29] M. M. Moghaddam, H. R. Ghazizadeh, and A. Mansouri, Commun. Nonlin. Sci. Numer. Simul. **14**, 3833 (2009).
[30] Z. Abbas and T. Hayat, Int. J. Heat Mass Trans. **51**, 1024 (2008).
[31] A. Mehmood, S. Munawar, and A. Ali, Commun. Nonlin. Sci. Numer. Simul. **15**, 4233 (2010).
[32] S. Munawar, A. Mehmood, and A. Ali, Chinese J. Phys. **50**, 828 (2012).